MICRORELAYS FOR BATCH TRANSFER INTEGRATION IN RF SYSTEMS

Veljko Milanović, Michel Maharbiz, Angad Singh, Brett Warneke, Ningning Zhou,
Helena K. Chan, Kristofer S. J. Pister
Berkeley Sensor and Actuator Center
497 Cory Hall #1770
University of California at Berkeley
Berkeley, CA 94720 - USA

ABSTRACT

This paper presents the first implementation of batch-transferred microrelays for a broad range of RF applications and substrates. The transferred relays include a variety of electrostatic pull-down type structures, as well as see-saw type structures. The batch-transfer methodology allows integration of optimized MEMS in RF systems on substrates such as sapphire, GaAs, and even CMOS. Gold-to-gold contact series microrelays with insertion loss of <0.15 dB, and isolation better than 36 dB at frequencies from 45 MHz to 40.0 GHz are demonstrated, as well as shunt switches with >40 dB of isolation and <0.12 dB insertion loss in that frequency range. A novel device structure which combines the benefits of see-saw operation and both shunt and series switching was shown to improve isolation of a single switch by ~8 dB while maintaining low insertion loss.

I. INTRODUCTION

Rapid growth of integrated circuit compatible micromachining technologies has spawned extensive research efforts in applications to wireless communications [1],[2]. The developments in microfabrication technology and MEMS have made possible the fabrication of actuators suitable for switching microwave signals. Consequently, miniaturization and integration of relays and switches for microwave applications has been the topic of extensive research [2]-[6]. Recent research efforts have been focused into lowering the operating voltages, improving insertion loss and isolation, lowering the cost of fabrication, achieving integration with present technologies, improving yield and reliability, as well as increasing the current-carrying capability.

More recently, there have been efforts in combining the flip-chip packaging technologies and MEMS in RF applications [7],[8]. In batch transfer integration methodology [9],[10], MEMS devices can be fabricated in a custom, optimized process, and transferred onto another substrate after release. The key advantage in RF systems is complete process decoupling - the MEMS structures are fabricated and optimized separately from the RF circuits and transmission lines, allowing integration of optimized MEMS in RF systems on substrates such as sapphire, GaAs, and even CMOS.

In our work, we demonstrate for the first time the feasibility of batch transfer integration of functional RF microrelays. This is demonstrated with simple electrostatic pull-down structures with isolated contact plates, similar to previously proposed switches [5]. Two types of pull-down structures were implemented – series type, where the contact plate connects the discontinued circuit when the structure is down; and the shunt type, where the contact plate shorts the transmission line when down. In both cases, the switches were designed for direct gold to gold contact, instead of capacitive switches [3], which are severely limited at lower frequencies (generally <10GHz). This allows operation down to dc, and well into millimeter wave frequencies, which is important in instrumentation applications such as power sensors [11],[12].

Along with the simple electrostatic pull-down structures, we implemented improved microrelays that utilize see-saw (pull-pull) type actuation which benefits from inherent bistability, and allows for lowering operating voltages and increasing OFF-state isolation. Namely, in simple pull-down switches, decreasing actuating voltages requires decreasing support beams' stiffness, which in turn makes the switches less mechanically stable (susceptible to acceleration and shock) and more vulnerable to stiction problems.

The see-saw devices are bistable in that they are electrostatically actuated in both states. Moreover, they do not rely on structural restoring forces to release metallic contact, hence allowing lower operating voltages while not compromising stability. As an additional consequence, we expect that these devices will be more reliable in long term operation.

II. FABRICATION OF THE DEVICES

In order to demonstrate the designed structures and batch transfer integration, we fabricated the MEMS devices on *donor* wafers, and the microwave structures on *target* wafers in separate processes. Both process flows, as well as the flip-chip batch transfer are schematically shown in Fig. I.

The microwave test structures are all based on coplanar waveguide (CPW) transmission lines, and were fabricated in gold (Cr/Au) on a quartz *target* wafer for low loss propagation well into millimeter wave frequencies. These simple test structures and CPW calibration sets were fabricated with a single metal

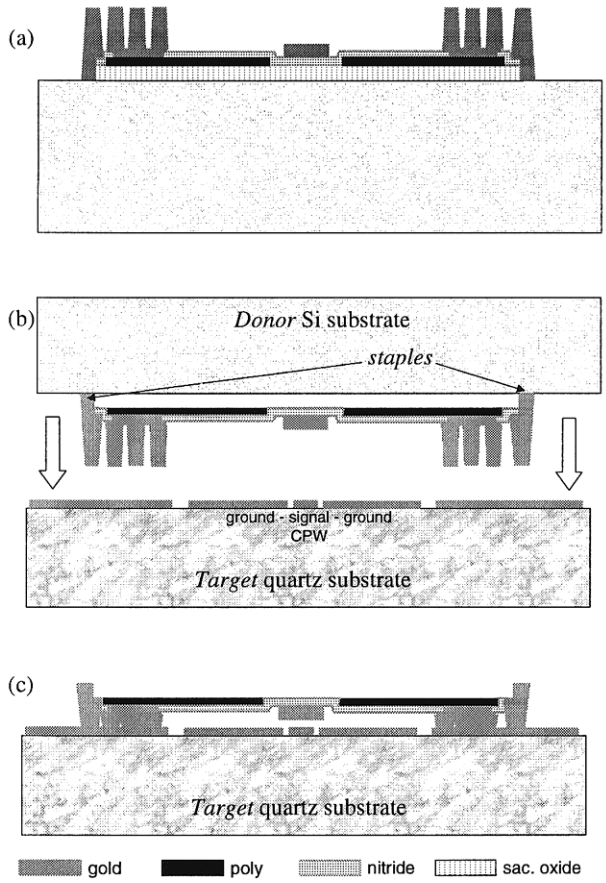

Figure I. Schematics of fabrication (a) example of structure before release and transfer, (b) after release, flipped and aligned for transfer onto target substrate, (c) final transferred structure.

mask. The wafers were then diced, cleaned and prepared for flip-chip transfer.

The MEMS devices were fabricated in the following four-mask process (Fig. Ia): starting with a p-type 100 mm silicon wafer (*donor* wafer), 0.6 μm of poly is deposited and patterned over 2 μm of sacrificial oxide. The poly features act as "pull-down" electrodes. Subsequently, 1 μm of low-stress nitride is deposited and patterned as the structural material. This layer of nitride acts as isolation for the poly pull-down plates as well, preventing shorting of the electrostatic plates in the finished relays. A 100Å/5000Å Cr/Au metal layer is subsequently evaporated and patterned as the relay contact plates (Fig. Ia). Another 150Å/600Å Cr/Au layer is evaporated as a seed layer; 6-8 μm gold bumps are then electroplated in a resist mold. At this point, donor wafers are diced. After resist-stripping, the structures on donor wafers are then released in concentrated in HF for ~4 minutes. The released structures remain on the individual chips due to the small gold bump *staples* [9], which were plated over the structures and surrounding silicon as shown in Fig. Ib. At that point, the devices are batch-transferred using a flip-chip bonder after careful alignment of *donor* and *target* chips, as illustrated in Fig. Ib. Although the process is designed for wafer-level transfers, at this time only chip-level transfers are considered and implemented. Details of the gold bump transfer process were given previously in [9],[10]. In short, the target and donor substrates are aligned and pressure is applied to form a gold-gold compression bond; the donor substrate is then removed, leaving the switches in place over the CPW lines (Fig. Ic). Application of greater pressure and temperature during transfer results in smaller distances between the structure and the target substrate, making these very important parameters in device integration.

The fabricated pull-down structures are shown in Fig. II. In Fig. IIa, the SEM micrograph shows the transferred relay on top of the CPW transmission line in Ground-Signal-Ground (GSG) configuration. The individual parts of the relay may be better seen in the microphotograph in Fig. IIb. The polysilicon pull-down plates extend from either anchored side over the ground planes of the CPW to maximize capacitance, thereby lowering actuation voltage. Over the signal strip of the CPW, only structural nitride and the gold contact plate are seen, designed to minimize parasitic effect on the CPW. The gold plate, seen in Fig. IIb is isolated by structural nitride and can make contact to the CPW below, either completing an open circuit in a *series* switch, or shorting the CPW strips in a *shunt* switch.

Fabricated see-saw type switches are shown in Fig. III. In Fig. IIIa, the concept of see-saw actuation is utilized to achieve a single-pole double-throw switch with a direct application in phase shifters [6]. At the top of Fig. IIIa, a CPW transmission line is divided into two arms, both of which are interrupted with series gaps giving isolation in the off state. After transfer, the see-saw switch is designed to connect either side of the divided CPW when actuation voltage is applied to the polysilicon plates on one or the other side of the structure. These switches were also implemented both in series and in shunt configurations.

Figure IIIb shows a SEM of a novel configuration see-saw switch which was designed to improve off-state isolation from single pull-down switches, while maintaining low insertion loss and additional mechanical benefits of the see-saw configuration. In this *series-shunt see-saw* structure, when the left/series side of the structure is pulled in, the CPW line is connected for low loss on-state. When the right/shunt side of the structure is pulled down, the series connection is removed, causing isolation in the transmission. Moreover, the shunt side shorts the CPW on the right side, thereby significantly increasing isolation.

III. DEVICE CHARACTERIZATION

A. Low frequency testing

The devices were tested by applying dc bias and observing the actuation and subsequent change in resistance in the CPW. On one chip, simple pull-down structures exhibited turn-on voltages between 25 V and 35 V, while the see-saw type structures exhibited lower pull-down voltages of 20 V. Thru resistance in the ON state for both series and shunt switches was measured at 0.3 Ω and 0.4 Ω, respectively. On many other chips,

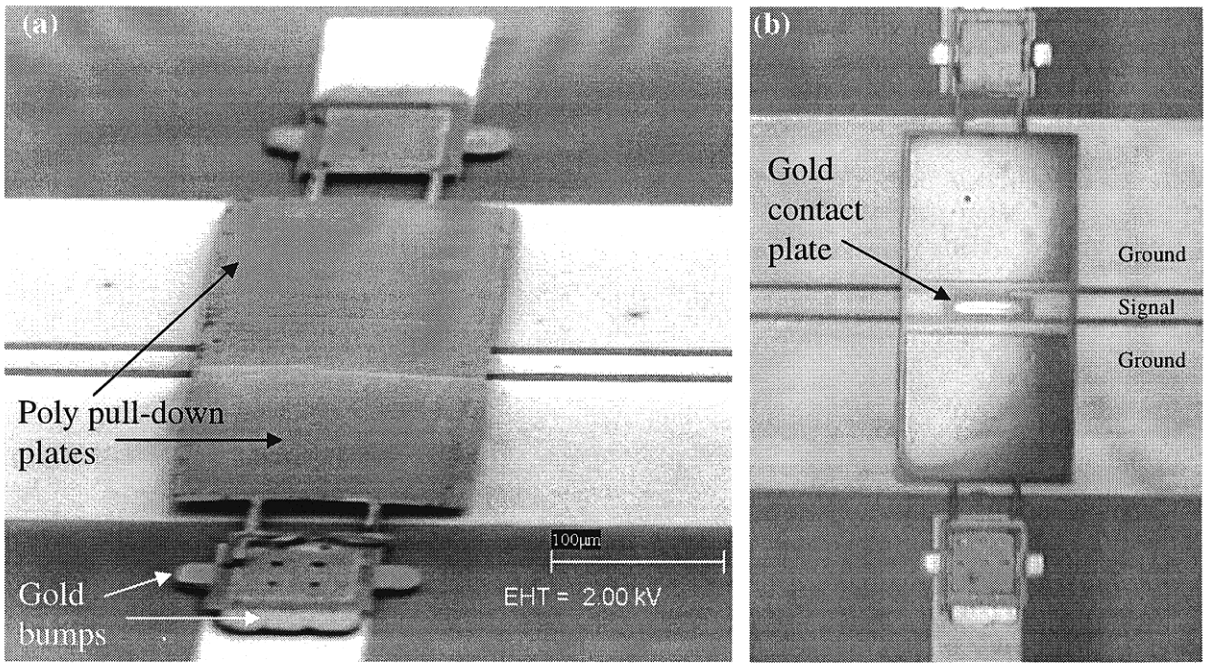

Figure II. Micrographs of electrostatic pull-down microwave switches batch transferred onto CPW transmission lines on a quartz substrate: (a) SEM of a typical device showing some bowing in the thin films and very good transfer alignment, and (b) an image of another device for series switching showing some misalignment in x and in y.

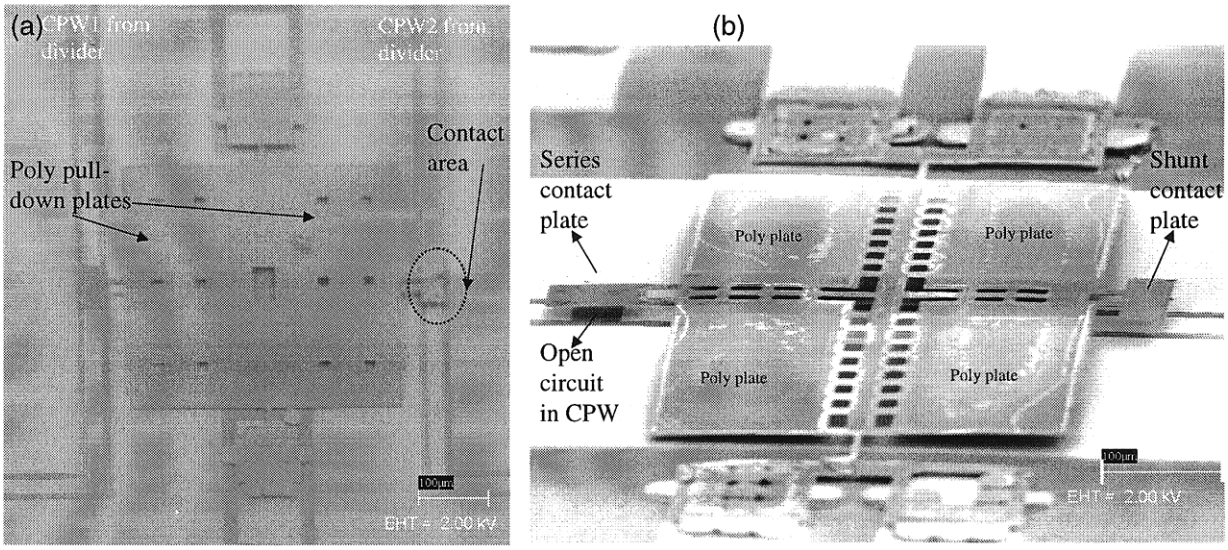

Figure III. Micrographs of see-saw type structures, (a) novel series-shunt microwave switch for improved isolation performance, and (b) single pole double throw see-saw switch for direct application in phase shifting networks.

however, pull-down voltages of 50 V to 60 V were observed. Finally, there were cases of chips on which over 110 V had to be applied to fully actuate the structures. These large variations in the pull-down voltage are believed to be due to the chip-to-chip variation in the height of the structures from the target chip due to variations in flip-chip transfer.

We characterized the transient response of the switches with a simple current measuring setup such that when relay plates were in contact, a current of 1 mA was flowing and the resulting voltage could be displayed on the oscilloscope. In Figure IV, a measurement of a pull-down device in room atmosphere is shown. Most of the devices tested exhibited turn-on times on the order of 200 μs, and turn-off times below 20 μs. The switch of Fig. IV was cycled over 200,000 times before failing, but more study of reliability of the devices is required.

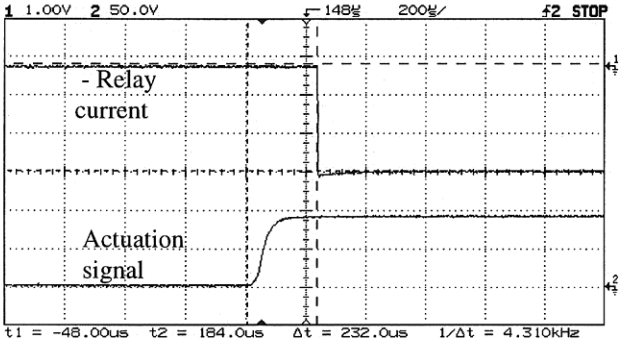

Figure IV. Measured switching response.

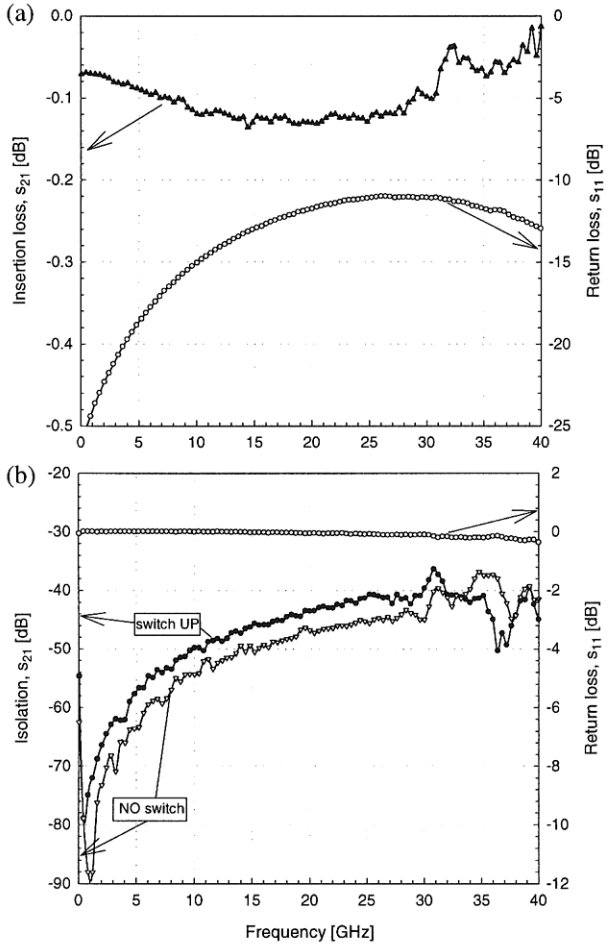

Figure V. Measured performance of a series pull-down microrelay (a) DOWN - gold contact plate completing the CPW transmission line, (b) isolation when UP.

B. Microwave testing

Microwave testing was performed using a vector network analyzer and a probe station at frequencies from 45 MHz to 40 GHz. Calibration and de-embedding was performed by measuring CPW transmission lines and reflects of different lengths on the same chip. After proper de-embedding [13], the measurement reference planes were brought just before the microrelays on the test structure CPW. With the calibration, we measured the insertion loss (s_{21} parameter) and the return loss (s_{11} parameter) while

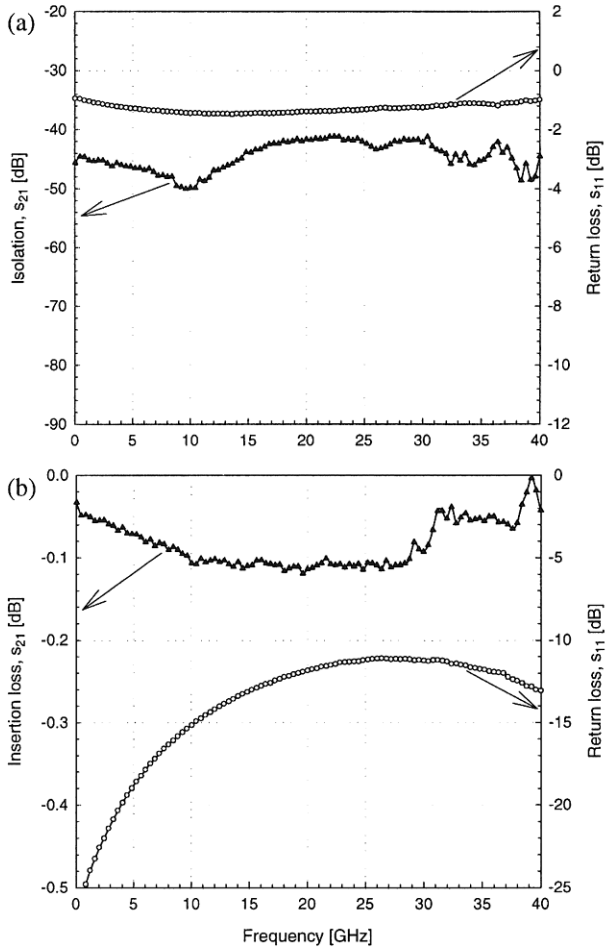

Figure VI. Measured performance of a shunt pull-down microrelay (a) DOWN - isolation with gold contact plate shorting the CPW transmission line, (b) insertion loss when UP.

switching the devices off and on with a dc voltage applied between the polysilicon pull-down plates and the CPW ground planes.

Firstly, we characterized the series pull-down switches (Fig. 2b) in which the gold contact plate completes the interrupted CPW signal strip when the switch is ON/DOWN. Figure Va shows the insertion loss and return loss in the ON state, and Figure Vb shows the same parameters in the OFF/UP state. In this relay, the CPW gap was 60 μm and the structure was approximately 4 μm above the CPW, resulting in high isolation (Fig. 5b) of better than 36 dB throughout the measured frequency range. Further, we tested shunt-type switches in which the gold contact plate shorts the CPW when the switch is down, resulting in isolation when actuated. Measured insertion loss and isolation is shown in Figure VI. In the OFF/UP state, very low insertion loss is seen due to the uninterrupted CPW in this type of switch. The loss is mainly due to parasitic electromagnetic coupling to the contact plate and nitride membrane above the CPW. In the ON/DOWN state the isolation was measured to be >40dB due to the relay's 40 μm wide shorting contact plate.

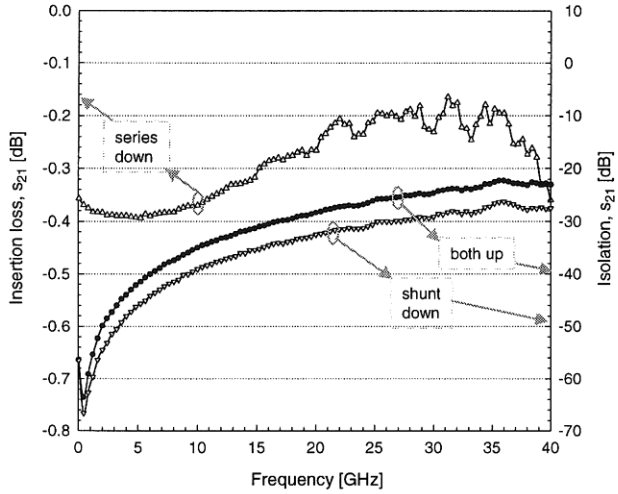

Figure VII. Measured performance of one series-shunt see-saw microrelay. Insertion loss is shown in the case of no actuation (both plates up), in the case of ON actuation (series plate down), and in the case of OFF actuation (shunt plate down.)

Measurements of see-saw series-shunt devices (Figure IIIb) presented more difficulty. In many variations of the design, there were problems with correct actuation of the structures due to the pull-down of the overall structure which will be discussed in more detail in Section IV. Some devices, however, behaved correctly, and results for such a relay are given in Figure VII. The relay was first measured in the idle state, i.e. with no applied voltages (both contact plates UP.) Isolation below ~22 dB was measured, which was expected due to the series gap of 30 μm (vs. 60 μm for Figure Vb.) With the shunt side actuated (25 µm wide contact plate), the isolation increased by ~ 8dB across the entire frequency range. Finally, in the ON state, with the series plate down, insertion loss <0.4 dB was measured.

IV. SIMULATION

To better understand the observed behavior of the structures, verify the trade-offs, and improve the designs for future fabrication, we performed simulations using SUGAR [14],[15].

Firstly, linear analysis was performed by using a linear beam model in which displacements are proportional to forces applied. From this analysis, which was done both in 2D and in 3D, we extracted pull-down voltages for both types of structures, as shown in Figure VIII. However, measurements of chips flip-chip transferred using lesser pressure (as discussed in Section II) exhibited significantly larger pull-down voltages at larger gap distances than predicted by linear model simulations. Namely, we measured pull-down voltages ranging from 25 V to 120 V, corresponding gap distances from approximately 1.5 µm to 10 µm based on SEM images. We attribute the discrepancy to the presence of axial forces and residual stresses in the structural materials, resulting in nonlinear effects. Larger plate deflections introduce greater non-linearities, as was the case in some structures where flip-chip transfer resulted in gap distances greater than ~2

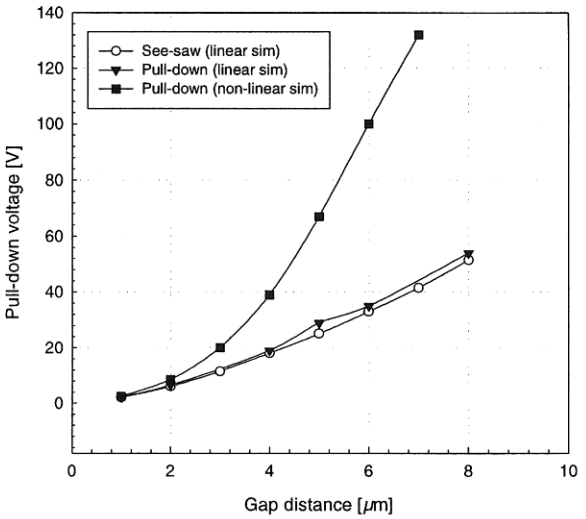

Figure VIII. SUGAR simulations pull-down voltage dependence on gap distance after batch transfer.

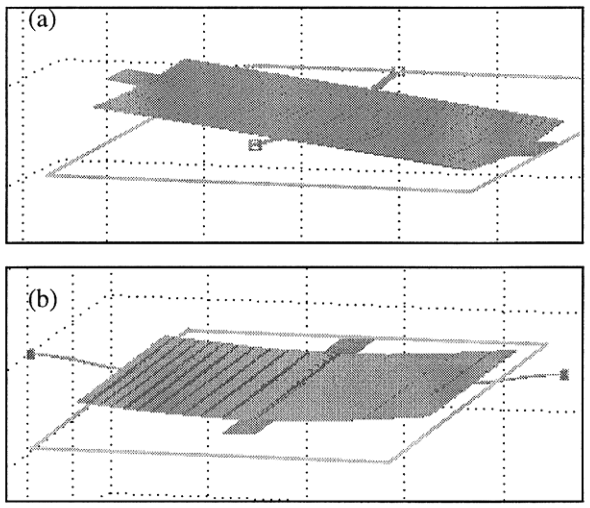

Figure IX. 3D SUGAR simulations of the see-saw structures: (a) structure tilting as desired, but undesired pull-down of the torsional beams visible, and (b) pull-down of torsional beams dominates the actuation, and both sides of the see-saw structure make contact simultaneously.

μm. In both pull-down and seesaw structures clamped-clamped beams (anchored at two ends) provide support. When pulled down, large tensile axial forces are present in the beams, causing nonlinear effects to dominate. Subsequently, a non-linear analysis in SUGAR of the simple pull-down structure that included the axial forces showed better agreement. Better modeling can be achieved by included the residual stresses and making more precise measurements of the gap.

Another important result from the 3D simulations of the see-saw type structures is demonstrated in Figure IX. Namely, while the desired actuation is only in the rotational (tilting) mode, the simulations clearly show the additional pull-down motion of the complete structure (Figure IXa). Moreover, there are cases in which the longer length of the torsional beams resulted

in complete contact of the structural plate (Figure IXb) instead of desired tilting. This was also observed experimentally - some structures contacted at both ends simultaneously.

As a result of the numerical and experimental study, we drew the following conclusions:

1) the pull-down motion introduces non-linearity which significantly increases pull-down voltages and sensitivity to variation in gap distances. Due to gap variation from the flip-chip transfer process, we need to eliminate this non-linearity.

2) achieving pull-down voltages below 10V will require very tight control of the transfer parameters and resulting gap distance.

3) we want to increase the electrostatic torque and decrease the bending by moving the polysilicon pull-down plates further away from the torsional centerline, increasing bending stiffness, and decreasing torsional stiffness.

V. Conclusion

We presented the design, fabrication, and batch-transfer integration of low-loss microrelays for microwave applications. Different types of switches were experimentally demonstrated, all based on polysilicon pull-down plates, structural/isolation nitride, gold bumps and gold-to-gold contacts. Their operation was characterized up to 40 GHz. One future goal is to extend the range of characterization frequencies and determine the upper frequency limit of operation. In addition, long-term reliability of the structures and gold-to-gold contacts will be studied more thoroughly, including operation at a variety of power ranges. Future designs will focus on reducing the actuation voltages, lowering contact resistances, and fabricating low-stress plates to prevent the detrimental bowing in the structures.

VI. Acknowledgement

The authors would like to thank Dana Teasdale, Mehmet Ozgur, and Lilac Muller for useful technical discussions. Measurements were performed at the High Speed Devices Group at University of California at San Diego, where authors want to thank Matt Wetzel, Rebecca Welty, and Peter Asbeck. Support for B. Warneke was provided by the Howard Hughes Doctoral Fellowship.

References

[1] C.T.-C. Nguyen, L.P.B. Katehi, G. M. and Rebeiz, "Micromachined devices for wireless communications," *Proceedings of the IEEE*, vol.86, no.8, p.1756-68, Aug. 1998.

[2] L. P. B. Katehi, G. M. Rebeiz, C. T.-C. Nguyen, "MEMS and Si-Micromachined Components for Low-Power, High-Frequency Communications Systems" *1998 IEEE MTT-S International Microwave Symposium Digest*, vol.4, p. 331-333, Jun. 1998.

[3] Z.J. Yao, S. Chen, S. Eshelman, D. Denniston, and C. Goldsmith, "Micromachined low-loss microwave switches," *Journal of Microelectromechanical Systems*, vol.8, no.2, pp.129-34, June 1999.

[4] D. Hyman, A. Schmitz, B. Warneke, T. Y. Hsu, J. Lam, J. Brown, J. Schaffner, A. Walston, R. Y. Loo, G. L. Tangonan, M. Mehregany, and J. Lee, "GaAs-compatible surface-micromachined RF MEMS Switches," *Electronics Letters,* vol.4, p.1507-10, June 1999.

[5] J. B. Muldavin, G. M. Rebeiz, "30 GHz Tuned MEMS Switches," *1999 IEEE MTT-S International Microwave Symposium Digest,* vol.4, p.1511-1514, June 1999.

[6] K. Suzuki, S. Chen, T. Marumoto, Y. Ara, and R. Iwata, "A Micromachined RF Microswitch Applicable to Phased-Array Antennas," *1999 IEEE MTT-S International Microwave Symposium Digest,* vol.4, p.1923-1926, June 1999.

[7] K. F. Harsh, W. Zhang, V. M. Bright, and Y. C. Lee, "Flip-Chip Assembly for Si-Based RF MEMS," Proceedings of the 12th IEEE International Conf. on Microelectromechanical Systems (MEMS `99), Orlando, FL, pp. 273-278, Jan. 1999.

[8] Z. Feng, W. Zhang, B. Su, K.F. Harsh, K.C. Gupta, V. Bright, and Y.C. Lee, "Design and modeling of RF MEMS tunable capacitors using electro-thermal actuators," *1999 IEEE MTT-S International Microwave Symposium Digest,* vol.4, p.1507-10, June 1999.

[9] M. M. Maharbiz, R. T. Howe, K.S.J. Pister, "Batch Transfer Assembly of Micro-Components On Surface and SOI MEMS," *Transducers '99*, Sendai Japan, June 7-10, 1999, pp.1478-81.

[10] M. M. Maharbiz, M. B. Cohn, R. T. Howe, R. Horowitz, A. P. Pisano, "Batch Micropackaging by Compression-Bonded Wafer-Wafer Transfer", *MEMS '99*, Orlando, FL, January 17-21, 1999, pp. 482-9.

[11] Hewlett-Packard Company, "Fundamentals of RF and Microwave Power Measurement," *Application Note AN 64-1A*, USA, Apr. 1997.

[12] V. Milanović, M. Gaitan, E. D. Bowen, N. H. Tea, and M. E. Zaghloul, "Thermoelectric Power Sensor for Microwave Applications by Commercial CMOS Fabrication," *IEEE Electron Devices Letters*, vol. 18, no. 9, pp. 450-452, Sep. 1997.

[13] R. B. Marks, "A Multiline Method of Network Analyzer Calibration," *IEEE Trans. on Microwave Theory and Tech.*, vol. 39, no. 7, pp. 1205-1215, July 1991.

[14] J. V. Clark, N. Zhou, K. S. J. Pister, "MEMS Simulation using SUGAR v0.5," *Solid-State Sensor and Actuator Workshop,* Hilton Head Isl., pp. 191-196, Jun. 1998.

[15] http://www-bsac.eecs.berkeley.edu/~cfm